frontiers | Frontiers in Energy Research

TYPE Original Research
PUBLISHED 04 March 2025
DOI 10.3389/fenrg.2025.1505654

OPEN ACCESS

EDITED BY
Liang Huang,
Chengdu University of Technology, China

REVIEWED BY
Peng Wu,
Dalian University of Technology, China
Changling Liu,
Qingdao Institute of Marine Geology (QIMG), China

*CORRESPONDENCE
Fugui Zhang,
375545821@qq.com
Shouji Pang,
271232645@qq.com

RECEIVED 03 October 2024
ACCEPTED 10 February 2025
PUBLISHED 04 March 2025

CITATION
Zhao C, Tang Y, Pang S, Zhang S and Zhang F (2025) Thermal released mercury: a new exploration technology for natural gas hydrate exploration in Tibetan Plateau permafrost area.
Front. Energy Res. 13:1505654.
doi: 10.3389/fenrg.2025.1505654

Thermal released mercury: a new exploration technology for natural gas hydrate exploration in Tibetan Plateau permafrost area

Chaoqing Zhao[1], Yu Tang[2], Shouji Pang[3]*, Shunyao Zhang[2] and Fugui Zhang[2,3]*

[1]China Liaocheng Bureau of Natural Resources and Planning, Liaocheng, China, [2]Institute of Geophysical and Geochemical Exploration, Chinese Academy of Geological Sciences, Langfang, China, [3]Observation and Research Station of Gas Hydrate and Permafrost Environment in Muli Town, Ministry of Natural Resources, Beijing, Qinghai, China

The occurrence environment and fundamental characteristics of natural gas hydrate (NGH) in the permafrost regions of the Tibetan Plateau are highly complex. A significant barrier to advancements in NGH exploration within these areas is the lack of effective exploration methods. The Juhugeng mining area represents the sole location in China's permafrost zone where NGH has been identified. In this study, we conducted a thermal released mercury (TRM) exploration experiment in the Juhugeng area, covering an area of 11.75 km^2 with a sampling density of 16 points per square kilometer. Soil samples were collected to a depth of 60 cm, totaling 163 samples, which were analyzed for TRM using the XG-7Z Zeeman mercury analyzer. The experimental results indicate that high-value anomalies of TRM occur at the boundaries of NGH deposits, while lower values are observed directly above the hydrates, forming an annular anomaly pattern. The maximum value of TRM recorded was 127.37 ngg^{-1}, with an average value of 32.59 ngg^{-1}, and the lower limit of the anomaly was established at 39.24 ngg^{-1}. By analyzing the spatial relationship between TRM anomalies and hydrocarbon anomalies, this study proposes a geogas migration mechanism for the formation of TRM anomalies. The anomalies are closely linked to NGH deposits, suggesting that TRM analysis is an effective auxiliary exploration technology for NGH in permafrost regions.

KEYWORDS

thermal released mercury, natural gas hydrate, exploration technology, permafrost region, Tibetan plateau

1 Introduction

Natural gas hydrate (NGH) is a crystal material formed from water and light gases (such as methane, ethane, propane, carbon dioxide, nitrogen, etc.,) under low temperature and high-pressure conditions (usually T is 0°C–10 °C, P > 10 MPa) (Sloan 2003). NGH is widely distributed in submarine sediments, terrestrial permafrost regions and deep-water lakes sediments (Kvenvolden 1993; Kvenvolden and Lorenson, 2001; Collett 1994; Collett et al., 2011; Zhu et al., 2010; Makogon et al., 2007). The total volume of CH_4 contained in NGH deposits is very large in comparison to other global CH_4 reservoirs, and the total recoverable volume is estimated to be ~3×10^{13} m^3 (Collett, 2002). Indeed, NGH has been proposed as a viable source of energy that could last throughout most of the 21st century

(Makogon et al., 2007). With the increasing need for energy and stricter requirements for the environment worldwide, every government attaches great importance to development and utilization of NGH (Boswell 2009; Collett et al., 2019). NGH is also the most important carbon pool in the shallow crust and is extremely sensitive to temperature and pressure changes (Kvenvolden 2022; Archer et al., 2009; Burton et al., 2020; Burton and Dafov, 2022; Burton and Dafov, 2023; Farahani et al., 2021).

The Tibetan Plateau is the largest permafrost area in the middle latitude zone of the earth, covering approximately about 150 × 10^4 km^2 and accounting for over 7% of the global permafrost (Zhou et al., 2000). Most permafrost regions possess conditions conducive to NGH formation, making this area a key focus for studying NGH in permafrost (Zhu et al., 2011). In 2008, the first NGH drilling was implemented in the Juhugeng mining area of the Qilian Mountain (Zhu et al., 2011; Lu et al., 2011; Zhang et al., 2021). This significant discovery marked the first detection of NGH in China's permafrost and in the low-middle latitude permafrost globally (Zhu et al., 2010; Lu et al., 2011). The Qilian Mountain permafrost regions are predominantly located in mid-latitude alpine zones, which differs significantly from the high-latitude permafrost areas around the Arctic Ocean where most of the NGH deposits are found. Compared to Arctic regions, the permafrost layers here are relatively thinner, and mean annual temperatures are higher (Zhou et al., 2000). This results in more complex mechanisms of hydrate formation, mineralization factors, and accumulation models in these regions (He et al., 2013; Zhai et al., 2014; Lu et al., 2015a; Lu et al., 2020; Zhang et al., 2020; Zhang et al., 2022).

In Arctic permafrost regions, the primary technologies for exploring NGH are seismic surveys and well logging, which have proven effective in locations such as Alaska's North Slope and the Mackenzie Delta (Schmitt et al., 2005; Riedel et al., 2009; Collett and Ehligio-Economides, 1983). The geological conditions of the Tibetan Plateau are complex, and low signal-to-noise ratio, difficulty in static correction, and poor imaging effects are challenges faced by seismic methods in the application of natural gas hydrate exploration (Fang et al., 2020; Fang et al., 2017). In the Qilian area, the content of NGH in rock layers is low (Wang et al., 2017), and the velocity of hydrate-bearing reservoirs is related to the lithology of the reservoirs and the degree of fracturing of the strata. Within the fault-broken zones, NGH appear in crystalline form (Wang et al., 2019), and the high-frequency scattered waves, after superposition, exhibit relatively high-frequency weak amplitude characteristics, without the Bottom Simulating Reflector (BSR) feature similar to that observed in marine seismic profiles (Fang et al., 2020; Ning et al., 2020). Although geophysical logging has identified the characteristics of NGH reservoirs as "high apparent resistivity, high P-wave velocity, low density, and low natural gamma," there are certain differences between different types of reservoirs, and the logging indicators are not sensitive enough (Lin et al., 2018; Fang et al., 2017; Ning et al., 2020). Geochemical technologies have emerged as a valuable complementary approach (Sun et al., 2014; Zhang et al., 2018; 2019; Tang et al., 2016; 2023; Zhou et al., 2021). However, traditional hydrocarbon indicators can be distorted by local coal deposits, complicating the accurate assessment of hydrocarbon sources.

Mercury (Hg) has become a crucial tool in geological research due to its vertical migration mechanisms, which are similar to those of oil and gas (Yang et al., 1995). Studies have shown that source rocks rich in organic matter tend to accumulate Hg and play a significant role in the migration and concentration of minerals involved in NGH formation (Yang et al., 1995; Xie 1992). Given its high volatility, Hg can easily penetrate overlying layers and permafrost, accumulating in surface soils. Thermal released mercury (TRM) is relatively unaffected by external disturbances, making the measured Hg content in soils closely related to deep hydrocarbon source rocks (Chen et al., 2001; Jia 2000). Therefore, Hg serves as an important indicator in oil and gas exploration. In the complex process of NGH formation, these hydrates, similar to petroleum and natural gas, also have the ability to accumulate Hg. Typically, hydrocarbon anomalies and TRM anomalies are found to coexist (Jia 2000; Lu et al., 2015b). TRM can effectively indicate the presence of NGH, thereby enhancing the success rate of geochemical exploration for these resources. This paper explores the relationship between TRM anomalies and hydrate deposits, aiming to further investigate the mechanisms underlying the formation of TRM anomalies in NGH.

2 Principle

Mercury (Hg), widely distributed in nature, is a crucial geochemical indicator in oil and gas exploration, characterized by its small atomic diameter (3.00×10^{-1} m), low water solubility, and high volatility (Li et al., 2008). Elemental mercury (Hg^0) is commonly found in natural gas (Leeper, 1981; Dai et al., 2001; Li et al., 2017; Zhang et al., 2019). The migration and accumulation of oil and gas represent dynamic equilibrium processes, often occurring in systems lacking perfectly sealed traps. Influenced by factors such as geothermal temperature, formation pressure, and concentration gradients, certain oil and gas components inevitably penetrate cap rocks and gradually migrate into overlying strata, ultimately reaching the surface. This phenomenon is known as vertical micro-leakage (Yang et al., 1995; Xie 1992). Elemental mercury (Hg^0), with a diameter smaller than that of methane and the effective diameter of water molecules, experiences minimal resistance during migration. Its extremely low solubility in water and weak chelation with water molecules further enhance its mobility. Mercury exhibits high vapor pressure and volatility, granting it significant penetrating ability. Its ions possess a relatively high ionization potential, making it readily reducible from various compounds to its elemental form. In the reducing environment of oil and gas reservoirs, mercury compounds are readily reduced to elemental mercury, which migrates upward along with elemental mercury already present in the reservoir. The migration mechanisms of hydrocarbons, the primary constituents of oil and gas reservoirs, also apply to mercury. The high mercury concentrations in oil and gas reservoir sources provide the material basis for its vertical migration. Concentration gradients and pressure differences are the primary driving forces and the fundamental control factors for migration. They determine the intensity and availability of surface oil and gas geochemical information. Faults and fractures, including micro-fractures, serve as the primary pathways for vertical migration. The distribution of faults and fractures dictates the distribution of anomalies in gas components, such as hydrocarbons and mercury, forming their distinct anomaly patterns (including bead-shaped, bay-shaped, semicircular, and ring-shaped, among others) in the plane (Yang et al., 2000). The sealing

capacity of oil and gas reservoir caps is pivotal in determining the migration pathways and mechanisms of gas components such as hydrocarbons and mercury. This, in turn, influences the migration volume and the spatial distribution of surface anomalies. Above oil and gas reservoirs, when the caprock exhibits good sealing properties, hydrocarbons predominantly migrate vertically through fractured pathways surrounding the reservoir via mechanisms such as filtration, dissolved hydrocarbons, and microbubbles. Their surface distribution typically forms a ring-shaped halo around the reservoir. In most cases, hydrocarbons primarily migrate vertically via filtration and diffusion, with surface anomalies taking the form of a block-shaped distribution directly above the reservoir. However, when the caprock has poor sealing properties, hydrocarbons, and gaseous components, such as mercury, migrate directly from above the reservoir to the surface through a combination of filtration, diffusion, and microbubble processes, resulting in irregular block-shaped surface anomalies. NGH share similar migration mechanisms and source characteristics with conventional oil and gas (Collett et al., 2009), enabling the application of TRM techniques from oil and gas exploration to investigate deep-seated NGH.

3 Study area

3.1 Geological setting

The study area is located within the Muli Coalfield in Tianjun County, Qinghai Province, at an elevation of 4,000 to 4,300 m. The region experiences an average annual temperature of −5.1°C and is characterized by widespread permafrost with an island-like distribution and an average thickness of 95 m (Zhu et al., 2006; Pan et al., 2008). Geologically, the area is part of a rift-graben basin formed by the reactivation of the northern Qilian deep fault system during the Yanshanian orogeny. Tectonically, it is situated within a depression zone between the central and southern Qilian structural units (Wen et al., 2010; Fu and Zhou, 2000) (Figure 1A). Hu indicates that the Cretaceous orogeny in the Qilian Mountains led to the region's early uplift. Significant tectonic and uplift events occurred during the early Eocene (53–40 Ma), late Eocene (~33 Ma), the Miocene (13–8 Ma), and the Pliocene, raising the Qilian Mountains to near their current elevation (Hu et al., 2017). By the end of the Pliocene, the range had reached the critical height required for glacial activity, with the Middle Pleistocene showing pronounced effects from global cooling and coupling influences (Hu et al., 2017).

The Juhugeng mining area is one of the main components of the Muli coalfield. Its central region consists of Triassic strata forming an anticline, while coal-bearing Jurassic strata create two synclines to the north and south (Wen et al., 2010; Fu and Zhou, 2000). Large-scale thrust faults are developed on both sides of the anticline, while significant NE-trending shear faults are present within the northern and southern synclines, segmenting the depression into discontinuous fault blocks (Lu et al., 2010). The area exhibits distinct structural characteristics, characterized by a north-south zonal and east-west sectional division (Figure 1B). The exposed strata in the Juhugeng mining area mainly consist of Quaternary, Middle Jurassic, and Upper Triassic formations. The Upper Triassic strata are prominently exposed in the northern and southern parts of the mining area, as well as along the axis of the anticline. These formations primarily comprise black siltstone, mudstone, and thin coal seams, exhibiting a parallel unconformity with the overlying Jurassic strata (Figure 1B). The Muli Formation, from bottom to top, consists of a sequence of medium-to coarse-grained clastic rocks formed in a braided river alluvial plain environment, occasionally interbedded with thin layers of carbonaceous mudstone or thin coal seams. The basal conglomerates are well-developed, transitioning to dark gray siltstone, fine-grained sandstone, and medium-grained sandstone, as well as coarse-grained sandstone formed in a lacustrine-swamp environment, with two main coal seams interbedded. The Jiangcang Formation, from bottom to top, consists of gray fine-grained sandstone, medium-grained sandstone, and dark gray mudstone and siltstone, deposited in a delta-lacustrine environment, containing 2 to six coal seams (Fu and Zhou, 2000; Hu et al., 2017; Pang et al., 2013). It transitions to fine clastic mudstone and siltstone formed in a shallow to semi-deep lake environment, interbedded with gray siltstone and lenticular siderite layers. The Quaternary strata are widely distributed in the drilling and consist of alluvial and diluvial humus, sand, gravel, colluvial breccia, and glacial deposits including mud, sand, ice layers, and erratic boulder.

3.2 Occurrence characteristics of NGH

Since 2008, the China Geological Survey has drilled 16 exploratory wells and 3 pilot production wells in the permafrost region of the Qilian Mountains. NGH were discovered in 9 of the exploratory wells and 2 of the pilot production wells, while the remaining exploratory wells exhibited only hydrate-related anomalies. Shenhua Qinghai Energy Co., Ltd. Has drilled 14 exploratory wells for NGH, with discoveries in 4 of these wells; the remaining wells showed only hydrate-related anomalies (Wang et al., 2019; Wen et al., 2015). Recent drilling investigations and laboratory studies have significantly clarified the fundamental geological characteristics of NGH.

In the permafrost region of the Qilian Mountains, NGH deposits are classified into two types. The first type, known as "fracture-type" hydrate, is visibly present as thin layers, platelets, or nodules within the fractures of siltstone, mudstone, and oil shale. These typically appear as white or milky white crystals, though some may appear yellow due to contamination from drilling mud. The second type, "pore-type" hydrate, is found as impregnations within the pores of fine siltstone. The crystals are not visible to the naked eye and must be inferred from indirect indicators such as the continuous emergence of gas bubbles and water droplets from core samples, or dispersed low-temperature anomalies detected by thermal infrared imaging. NGH are distributed within a depth range of 140–330 m and have a thickness of nearly 200 m (Wang et al., 2019), which is relatively shallow compared to polar permafrost regions. The vitrinite reflectance (*Ro*) of the source rocks ranges from 0.78% to 1.1%, with the maximum pyrolysis peak temperature (*Tmax*) reaching 470°C, indicating that the source rocks are in a stage of thermal maturation where significant oil and gas generation occurs. The methane content in the hydrate layers ranges from 54% to 76%, ethane from 8% to 15%, and propane from 4% to 21%, with minor amounts of butane, pentane, and other hydrocarbons. The CO2 content generally ranges from 1% to 7%, with some samples reaching up to 15%–17%. The spectral curves of the hydrates are similar to those of deep-sea hydrates from the Gulf of Mexico, classifying them as Type II hydrates. Carbon

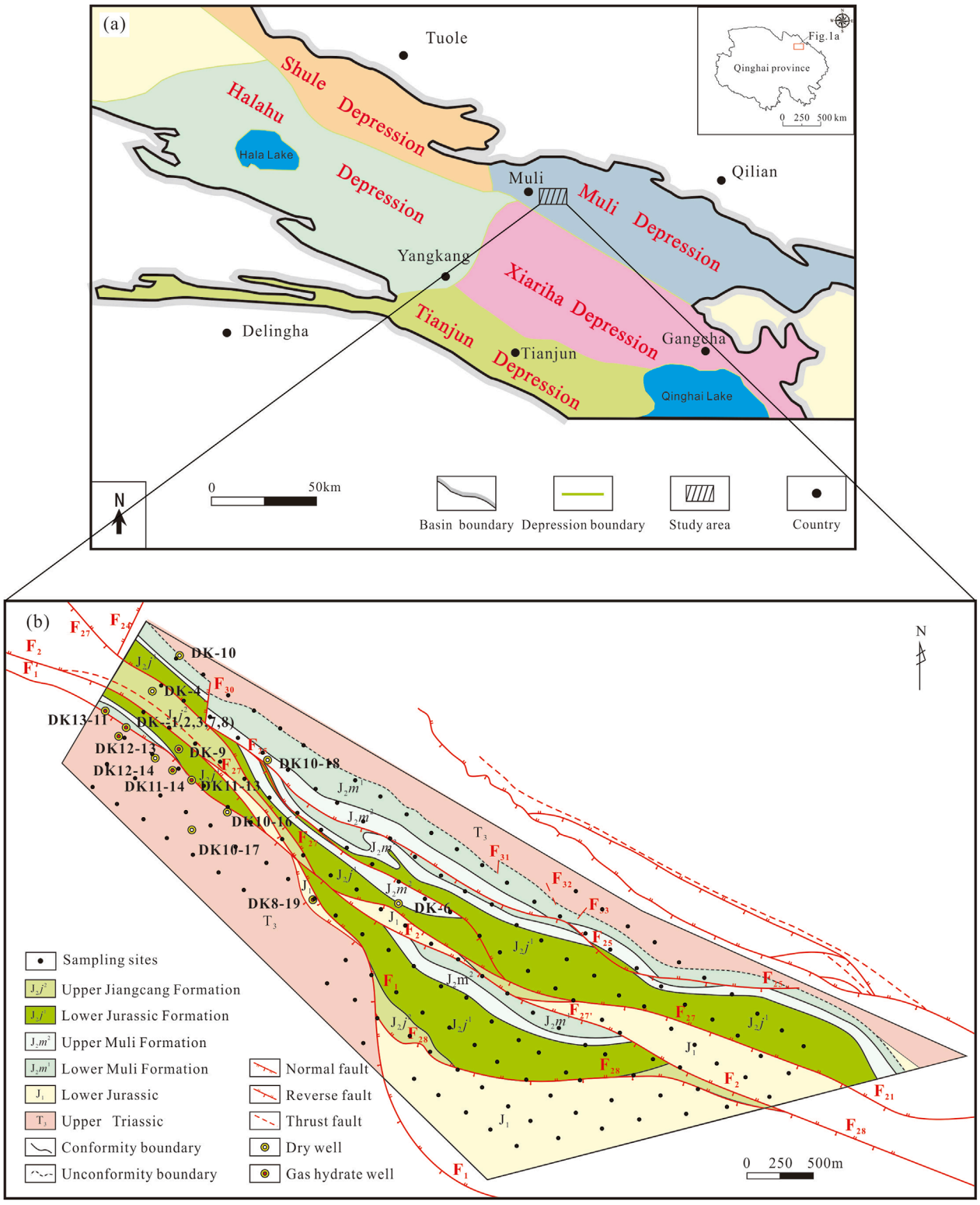

FIGURE 1
(A) Schematic map of the Southern Qilian Basin showing the distribution of tectonic units and the location of the Scientific Drilling Project of gas hydrate (modified from Fu and Zhou, 2000). **(B)** Geological map for the study area in the Qilian Mountain permafrost (modified from Wang et al., 2015).

isotope studies indicate that the gas sources for the NGH in the Qilian Mountains primarily originate from deeper formations. The gas generated in these source rocks migrates along faults to shallower levels, where it accumulates either directly or indirectly due to late-formed compressional faults blocking the gas. Since the late Pleistocene glaciations, this gas has either formed hydrates or remained in the strata as free or adsorbed gas (Zhang et al., 2022).

3.3 Distribution characteristics of NGH

Permafrost is a necessary condition for the formation of terrestrial NGH. The long-term real-time temperature monitoring results from the DK-9 well indicate that the geothermal gradient within the permafrost layer is 1.38°C per 100 m, while the geothermal gradient below the permafrost layer is 4.85°C per 100 m. Based on the temperature-pressure conditions for hydrate stability, the depth of the stability zone's lower boundary is between 510 and 617 m (Wang et al., 2017). The study area possesses favorable conditions for the formation of NGH. The drilling results show that the main gas hydrate bearing horizon is the Middle Jurassic Jiangcang Formation, located beneath the permafrost layer. The primary reservoir intervals are between depths of 133.0–396 m (Wang et al., 2015). The vertical distribution of NGH in the wells is discontinuous, and there is no clear lateral distribution pattern between wells. The rock fracture system plays a significant controlling role in the distribution of NGH (Wang et al., 2011). NGH are found beneath the permafrost layer, and no gas hydrates or their associated anomalies have been observed within the permafrost layer (Wang et al., 2015). There is a significant variation in the estimated gas hydrate saturation range. The average hydrate saturation in sandstone pores is 5.1% (Lu et al., 2011), while the saturation ranges calculated from logging data are 1.3%–8.6% and 11.47%–81.61% (Guo and Zhu, 2011; Lin et al., 2018), with relatively similar results. However, when selecting saturation calculation models, certain assumptions are made, and further work is required, including rock physics experiments, petrophysical testing, and formation water analysis (Lin et al., 2017).

4 Materials and methods

A methodological trial was conducted in the known NGH area of the Juhugeng region in the Qilian Mountains, with sampling carried out from June to August 2013. The survey area covered 11.75 km^2 with a sampling density of 16 points per square kilometer. Soil samples were collected at depths of 40–60 cm (Sun et al., 2014), and totaling 163 samples, each wrapped in glassine paper. In the laboratory, the samples were air-dried and processed to a particle size of 80 mesh.

Before testing the laboratory samples, 50 mg of each of the six national primary standard materials (GSS-11, GSS-14, GSS-18, GSS-20, GSS-26, and GSS-27) were accurately weighed and injected into mercury recovery tubes with a recovery rate greater than 85%. The mercury concentration was determined by a mercury analyzer (XG-7Z Zeeman Mercury Analyzer, Institute of Geophysical and Geochemical Exploration, Chinese Academy of Geological Sciences, China), with absorbance values measured. The relative standard deviation was required to be less than 3%. A standard calibration curve was plotted with absorbance as the vertical coordinate and the amount of standard mercury injected as the horizontal coordinate. The instrument was preheated for 30 min until it stabilized. Fifty milligrams of the prepared sample were placed in a quartz boat, which had been purified, and then positioned in the pyrolysis furnace. The furnace temperature controller was activated to heat the quartz furnace from room temperature at a rate of 20°Cmin^{-1}, reaching 800°C within 40 min. During this process, air was used as the carrier gas, with a flow rate of 1.2–1.5 Lmin^{-1} to continuously extract mercury vapor into the absorption chamber for analysis. Simultaneously, a paperless recorder was employed to record both the temperature and absorbance.

The analytical testing for this study was conducted by the Central Laboratory of the Institute of Geophysical and Geochemical Exploration, Chinese Academy of Geological Sciences. In addition to conventional quality control measures, such as blank monitoring and instrument calibration with standard samples, the laboratory implemented management sample monitoring, duplicate blind sample monitoring, and re-testing of abnormal points to ensure data quality. The reporting rate for all testing indicators exceeded 90%, with a relative error of less than 20%. The pass rate for control samples was above 86.67%, meeting both regulatory standards and design requirements.

5 Results and discussion

5.1 Concentration of hg

Hg is highly volatile, and during the heating process in the TRM method, both inorganic and organic Hg in the soil is converted into Hg vapor, which may mix with Hg related to oil and gas. The presence of Hg unrelated to oil and gas can introduce significant biases in the application of TRM. In geochemical exploration for oil and gas, considering the total Hg (THg) content can help mitigate the interference affecting TRM indicators. In soil samples, locations where TRM levels are high while THg levels are relatively low can be identified as anomaly points associated with micro-leakage of oil and gas. The statistical results for TRM and THg are presented in Table 1. The minimum TRM value is 5.9 ngg^{-1}, the maximum is 127.37 ngg^{-1}, and the average is 32.59 ngg^{-1}, with a coefficient of variation of 0.66. For THg in soil, the minimum value is 10 ngg^{-1}, the maximum is 317 ngg^{-1}, and the average is 83.40 ngg^{-1}, with a coefficient of variation of 0.63.

5.2 Anomalies distribution characteristics

Figure 2 presents the contour map of soil TRM, identifying an anomalous lower limit of 39.24 ngg^{-1} using a dual-logarithmic approach with frequency and concentration. A low-value anomaly is observed above the NGH deposits, where the thickness of the permafrost exceeds 65 m, meeting the temperature and pressure conditions necessary for hydrate formation. Exploration wells DK-4, DK-10, DK10-16, DK10-17, and DK10-18 were found to be dry, marking the boundary of the hydrate, while high-value anomalies in soil TRM correspond to this hydrate boundary, consistent with the findings from the exploration wells. Based on geochemical exploration results, including the current soil

TABLE 1 The content of TRM and THg in surface soil.

Indicator	Maximum	Minimum	Mean	Coefficient of variation
TRM ($ng \cdot g^{-1}$)	127.37	5.91	32.59	0.66
THg ($ng \cdot g^{-1}$)	317.01	10.02	83.43	0.63

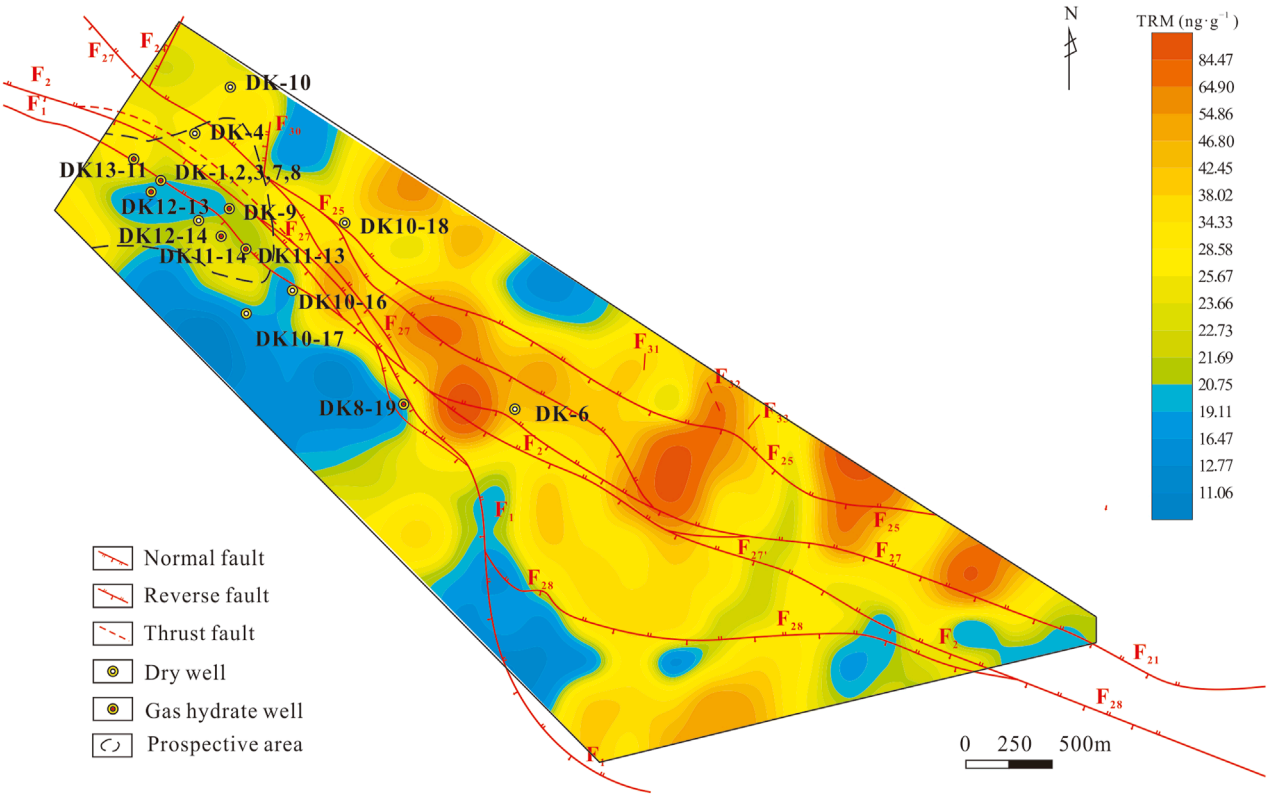

FIGURE 2
Geochemical anomalies and tectonic map of TRM in Juhugeng aera.

TRM survey, four additional wells—DK-9, DK13-11, DK12-13, and DK11-14—were strategically placed in favorable hydrate zones, all of which confirmed the presence of NGH (Figure 2).

The collected samples were also tested for acid-soluble hydrocarbons, analyzing the concentrations of hydrocarbon components from C_1 to C_5. This study utilized data on acid-soluble methane and heavy hydrocarbons, conducting initial analyses using EXCEL software. Through frequency grouping and examination of data distribution characteristics, the data were divided into 15 logarithmic intervals. The kriging method was then employed for interpolation, resulting in the creation of geochemical maps.

Figures 3, 4 present the geochemical maps for soil acid-soluble methane and heavy hydrocarbons, respectively. The distribution of acid-soluble methane and heavy hydrocarbons exhibits both similarities and differences when compared to the anomalies in soil TRM. These variations are primarily reflected in the following aspects: (1) The correlation between acid-soluble methane and heavy hydrocarbons is notably high (R^2 = 0.6614), indicating a common origin. In the northwest coalfield region and directly above the NGH deposits, both exhibit anomalous distributions. The higher concentrations in the coalfield area are attributed to coalbed methane (Zhang et al., 2022). Conversely, the acid-soluble hydrocarbon anomalies above the NGH deposits are a result of hydrocarbon migration associated with the hydrates, suggesting that these anomalies could serve as indicators of NGH reservoirs. (2) The acid-soluble hydrocarbon anomalies display an annular pattern in areas where NGH are anomalous. Similarly, the soil TRM also shows an annular anomaly, indicating a high degree of overlap between the two. Both anomalies are characterized by large areas and high intensities, reinforcing their correlation. (3) In the southeastern part of the study area, anomalies in soil acid-soluble hydrocarbons, including methane and heavier hydrocarbons, correspond to the annular anomalies in soil TRM. This correlation indicates that the area could be a priority target for NGH exploration. The presence of TRM can serve as an auxiliary indicator to enhance the success rate of hydrocarbon exploration. (4) The central part of the study area exhibits significant TRM anomalies, which are attributed to the active geological gas migration associated with fault development in

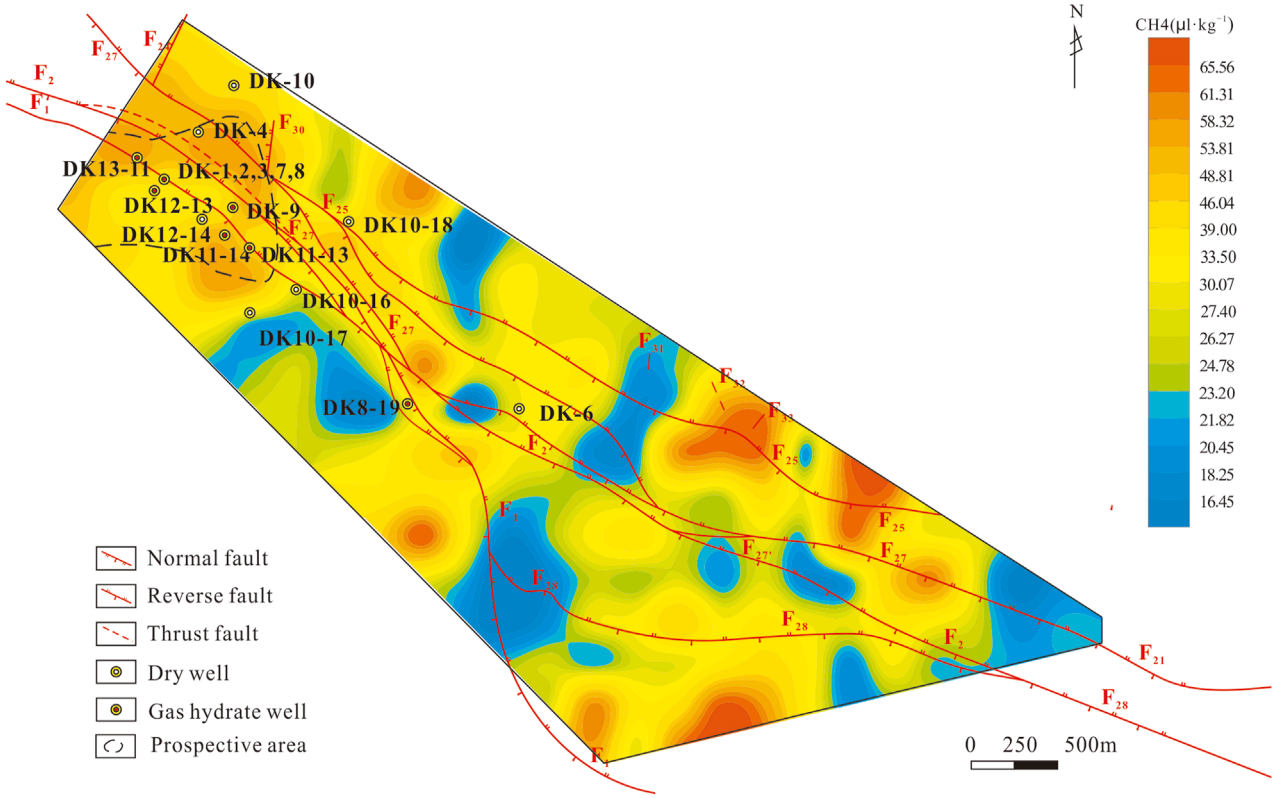

FIGURE 3
Geochemical anomalies map of acid extracted methane in Juhugeng area.

the region. In this area, the intensity of acid-soluble hydrocarbon anomalies, particularly methane, is relatively low, suggesting a reduced likelihood of NGH formation.

5.3 Fractal characteristics of TRM

Fractal theory, which is defined by characteristics such as fractal dimensions, self-similarity, statistical self-similarity, and power-law distributions, has been applied in the field of geology (Li and Ma, 1999; Cheng et al., 1994). It provides an effective approach for uncovering the spatiotemporal structural features of mineralization systems (Cheng, 1999; Cheng, 2001; Shen, 2002; Li and Cheng, 2004; Zuo and Wang, 2015). This approach enables geoscientists to explore the complex, often non-linear patterns in geological formations, enhancing our understanding of the processes that govern resource distribution and refining exploration technologies.

The fractal statistical model is Formula 1.

$$N(r) = Cr^{-D}, r > 0 \quad (1)$$

where r denotes the content of TRM; C is the proportional constant, which is >0; D is the fractal dimension, which is >0, and $N(r)$ represents the amount of He, Ne, and CH_4 in the drill core headspace gas with content equal to or greater than r. This fractal statistical model effectively captures the overall spatial structural characteristics of geochemical anomalies. By taking the logarithm of both sides of the fractal statistical model for TRM in soil, the equation can be transformed into a simple linear regression Formula 2:

$$lg[N(r)] = -Dlg(r) + lg(C), r > 0 \quad (2)$$

Figure 5 presents the fractal plot of TRM in soil, constructed by plotting the Hg concentration against its frequency in a scatter diagram. The fractal dimension (D) of the regression model was determined using the least squares method. From the figure, it can be observed that: (1) The TRM in the soil exhibits a multifractal nature, with fractal dimensions $D_1 = 0.292$, $D_2 = 1.537$, $D_3 = 2.260$, and $D_4 = 2.835$ (Table 2). The lower fractal dimension in the first layer indicates a region with lower values near the detection limit, reflecting the geochemical distribution of the original TRM in the soil. (2) The fractal dimension of the second layer is also relatively low, indicating a narrow range of concentrations coupled with a higher frequency, which reflects the background levels of TRM in the soil. (3) The third layer exhibits a larger fractal dimension, with an expanded concentration range and a lower frequency. This indicates the presence of anomalies in TRM, reflecting the geochemical distribution associated with gas migration. (4) The fourth layer has the highest fractal dimension, the largest concentration range, and the lowest frequency. This suggests the presence of localized high anomaly values in TRM, reflecting the geochemical distribution characteristics associated with leakage along fractures in the soil. (5) The multifractal distribution of TRM in the Juhugeng area not only reveals the distribution patterns influenced by various geological processes at different levels, but also establishes the lower limit for elemental anomalies. The lower limit determined through this fractal

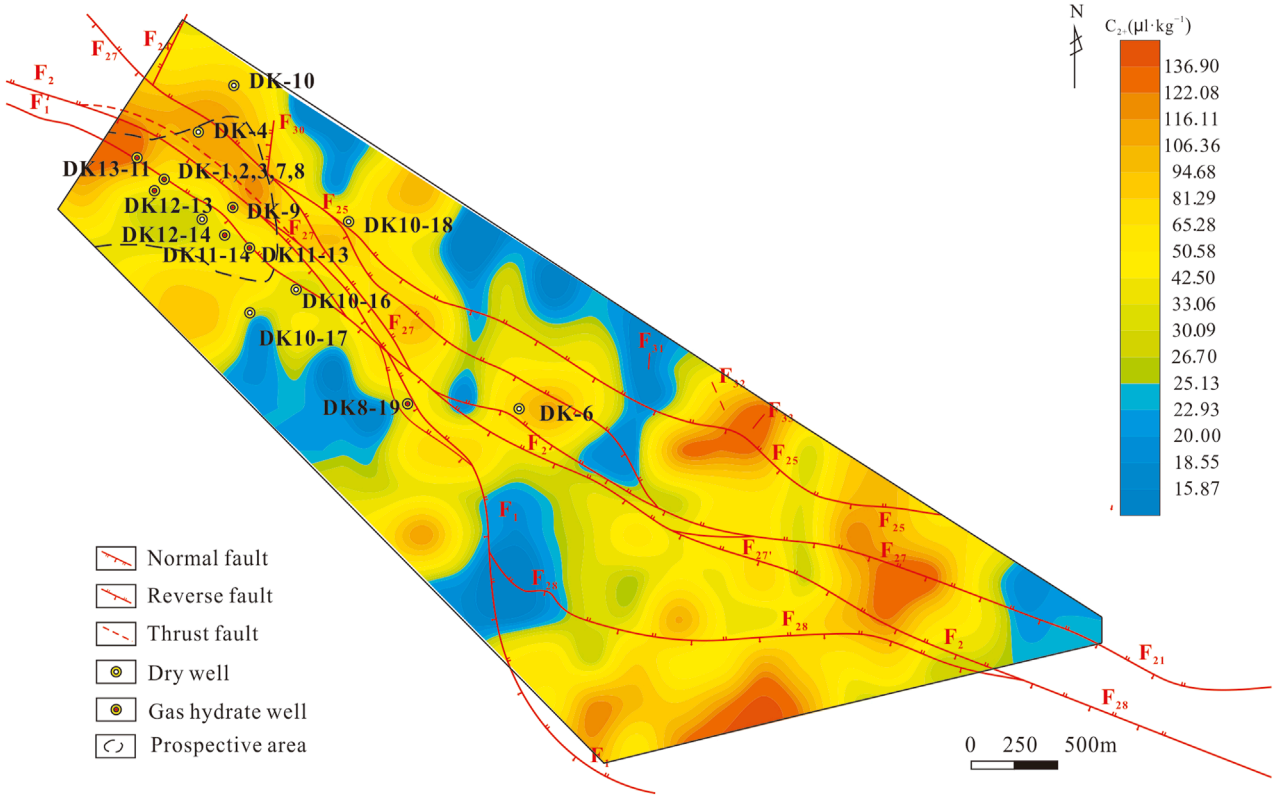

FIGURE 4
Geochemical anomalies map of acid extracted heavy hydrocarbons in Juhugen area.

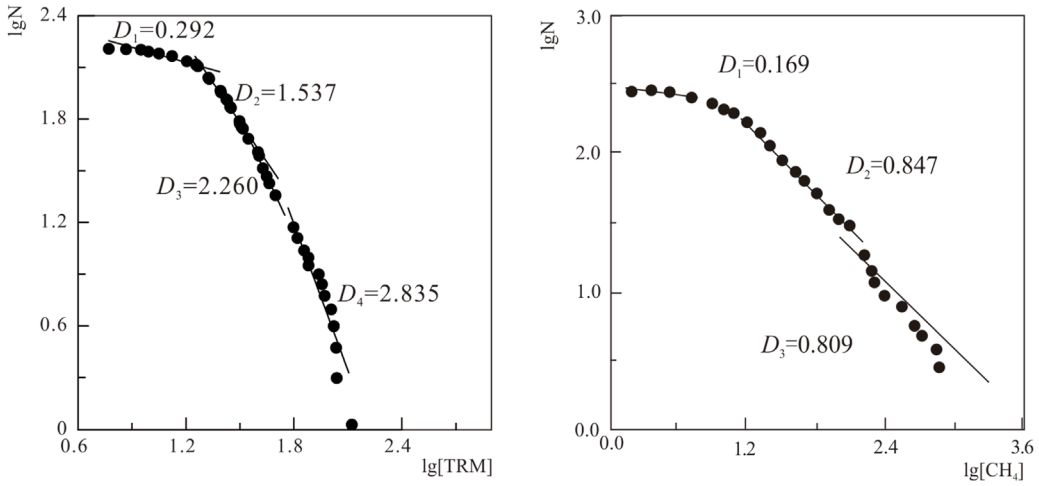

FIGURE 5
Fractal graphs of soil TRM and methane in Juhugeng area.

analysis is 39.24 ngg^{-1} (Table 2). (6) The fractal dimensions D1, D2, and D3 of methane are 0.169, 0.847, and 0.809, respectively. Methane is multifractal and the fractal dimension is comparatively small, which indicates that various geochemical processes such as microleakage and microbial oxidation occur during the vertical migration of methane.

5.4 Geogas migration mechanism of hg

In permafrost regions, NGH can be divided into four distinct zones: the source rock layer, the NGH layer, the permafrost layer, and the seasonal permafrost layer. The source rock layer is rich in

TABLE 2 The characteristics statistics of TRM fractal in Juhugeng area.

Analysis level	Multifractal dimension (*di*)	Concentration range ($ng \cdot g^{-1}$)	Sample size	Boundary point (r_{i0})
1	0.292	5.90–19.48	44	$r_{12} = 19.48$
2	1.537	19.97–39.24	79	$r_{23} = 39.24$
3	2.260	39.82–55.04	25	$r_{34} = 55.04$
4	2.835	58.56–127.37	15	

organic matter and serves as a stable source of methane for the formation of NGH. The hydrocarbons in the source rocks migrate upward, providing the necessary methane for hydrate formation. The NGH layer refers to the stratum where NGH are stored. Hydrocarbons migrating upward from deeper oil and gas reservoirs undergo geochemical differentiation, with some forming NGH. Hg ions, with their small ionic radius and high geochemical activity, can easily penetrate overlying rock and permafrost layers. This results in the formation of geochemical anomalies above the hydrate deposits, as Hg accumulates in the overlying layers. The permafrost layer extends from the surface's seasonally thawed layer to the base of the permafrost. It remains frozen for extended periods, which suppresses conventional geochemical reactions. However, soil gas migration remains active, allowing Hg and other trace elements to move upward with the gas flow and accumulate near the surface. The seasonal thaw layer refers to the near-surface zone that undergoes periodic freezing and thawing. Within this layer, soil organic carbon and minerals such as quartz, feldspar, illite, and kaolinite actively absorb Hg migrating from deeper layers.

The geogas migration mechanism of TRM is intricate. It involves factors such as the amount of Hg absorbed during the formation of the hydrate, the vertical migration of hydrocarbons through the permafrost, and the infiltration and enrichment of Hg. Compared to the surrounding environment, Hg concentrations in NGH deposits show noticeable differences. By integrating this data with other geophysical and geochemical exploration methods, it becomes possible to delineate and predict favorable areas for NGH exploration.

6 Conclusion

Moderate-intensity TRM anomalies were detected above the NGH deposits in the Juhugeng area of the Qilian Mountains. Ten wells—DK-1, DK-2, DK-3, DK-7, DK-8, DK-9, DK13-11, DK11-14, DK12-13 and DK11-13—where NGH were discovered, are all situated within this anomaly zone. By integrating hydrocarbon anomalies, permafrost distribution, and fault-controlled structures, TRM anomalies can serve as a supplementary tool for NGH exploration, significantly enhancing the detection success rate for NGH. This research demonstrates a strong correlation between TRM anomalies and NGH, showing good consistency with hydrocarbon indicators. Since TRM reflects the long-term integrated effects of hydrocarbon migration and seepage, the information is relatively stable and less affected by surface conditions. Thus, it has considerable potential to be promoted as a key technology for NGH exploration.

Data availability statement

The original contributions presented in the study are included in the article/supplementary material, further inquiries can be directed to the corresponding authors.

Author contributions

CZ: Conceptualization, Writing–original draft. YT: Investigation, Writing–review and editing. SP: Writing–review and editing, Conceptualization, Resources. SZ: Investigation, Writing–review and editing. FZ: Conceptualization, Writing–review and editing.

Funding

The author(s) declare that financial support was received for the research, authorship, and/or publication of this article. This study was financially supported by the open fund project of the Observation and Research Station of Gas Hydrate and Permafrost Environment in Muli Town (Qinghai Province), Ministry of Natural Resources (No. 2024231), the National geological survey project of China (DD20243230) and the Science and Technology Innovation Project of Oil and Gas Survey, China Geological Survey (2023YC06).

Conflict of interest

The authors declare that the research was conducted in the absence of any commercial or financial relationships that could be construed as a potential conflict of interest.

Generative AI statement

The author(s) declare that no Generative AI was used in the creation of this manuscript.

Publisher's note

References

Archer, D., Buffett, B., and Brovkin, V. (2009). Ocean methane hydrates as a slow tipping point in the global carbon cycle. *Proc. Natl. Acad. Sci.* 106, 20596–20601. doi:10.1073/pnas.0800885105

Boswell, R. (2009). Is gas hydrate energy within reach? *Science* 325, 957–958. doi:10.1126/science.1175074

Burton, Z., and Dafov, L. N. (2022). Testing the sediment organic contents required for biogenic gas hydrate formation: insights from synthetic 3-D basin and hydrocarbon system modelling. *Fuels* 3, 555–562. doi:10.3390/fuels3030033

Burton, Z., and Dafov, L. N. (2023). Salt diapir-driven recycling of gas hydrate. *Geochem. Geophys. Geosystems* 24, e2022GC010704. doi:10.1029/2022GC010704

Burton, Z., Kroeger, K. F., Hosford Scheirer, A., Seol, Y., Burgreen-Chan, B., and Graham, S. (2020). Tectonic uplift destabilizes subsea gas hydrate: a model example from Hikurangi margin, New Zealand. *Geophys. Res. Lett.* 47, e2020GL087150. doi:10.1029/2020GL087150

Chen, Y. R., Dai, T. G., Zhuang, X. R., and Zhou, Q. M. (2001). Main controlling factors of vertical migration of gas components such as hydrocarbon and mercury. *Chin. Geol.* 28 (8), 28–32. doi:10.3969/j.issn.1000-3657.2001.08.005

Cheng, Q., Agterberg, F. P., and Ballantyne, S. B. (1994). The separation of geochemical anomalies from background by fractal methods. *J. Geochem. Explor.* 51 (2), 109–130. doi:10.1016/0375-6742(94)90013-2

Cheng, Q. M. (1999). Multifractality and spatial statistics. *Comput. and Geosciences* 25 (9), 949–961. doi:10.1016/s0098-3004(99)00060-6

Cheng, Q. M. (2001). Multifactal and geostatistic methods for characterizing local structure and singularity properties of exploration geochemical anomalies. *Earth Science-Journal China Univ. Geosciences* 26 (2), 55–60. doi:10.3321/j.issn:1000-2383.2001.02.010

Collett, T. S. (1994). Permafrost-associated gas hydrate accumulations[a]. *Ann. N. Y. Acad. Sci.* 715, 247–269. doi:10.1111/j.1749-6632.1994.tb38839.x

Collett, T. S. (2002). Energy resource potential of natural gas hydrates. *AAPG Bull.* 86, 1971–1992. doi:10.1306/61eeddd2-173e-11d7-8645000102c1865d

Collett, T. S., Boswell, R., Waite, B. W., Kumar, P., Roy, S. K., Chopra, K., et al. (2019). India national gas hydrate program expedition 02 summary of scientific results: gas hydrate systems along the eastern continental margin of India. *Mar. Pet. Geol.* 108, 39–142. doi:10.1016/j.marpetgeo.2019.05.023

Collett, T. S., and Ehligio-Economides, C. A. (1983). Detection and evaluation of the in-situ natural gas hydrates in the north Slope region, Alaska. Soc. Pet. Eng. *AIME, Pap. (United States)*. SPE 11673. doi:10.2118/11673-MS

Collett, T. S., Johnson, A. H., Knapp, C. C., and Bosewell, R. (2009). Natural gas hydrates: a review. *AAPG Mem.* 89, 146–219.

Collett, T. S., Lee, M. W., Agena, W. F., Miller, J. J., Lewis, K. A., Zyrianova, M. V., et al. (2011). Permafrost–associated natural gas hydrate occurrences on the Alaska North Slope. *Mar. Petroleum Geol.* 28 (2), 279–294. doi:10.1016/j.marpetgeo.2009.12.001

Dai, J. K., Ni, Y. Y., Huang, S. P., Peng, W. L., Han, W. X., Gong, D. Y., et al. (2017). Genetic types of gas hydrates in China. *Pet. Explor. Dev.* 44 (6), 837–848. doi:10.11698/PED.2017.06.01

Fang, H., Xu, M. C., Lin, Z. Z., Zhong, Q., Bai, D. W., Liu, J. X., et al. (2017). Geophysical characteristics of gas hydrate in the Muli area, Qinghai province. *Nat. Gas. Sci. Eng.* 37, 539–550. doi:10.1016/j.jngse.2016.12.001

Fang, S. N., Lin, Z. Z., Zhang, Z. S., Zhang, C. M., Pan, H. P., and Du, T. (2020). Gas hydrate saturation estimates in the Muli permafrost area considering Bayesian discriminant functions. *Pet. Sci. Eng.* 195, 107872. doi:10.1016/j.petrol.2020.107872

Farahani, M. V., Hassanpouryouzband, A., Yang, J. H., and Tohidi, B. (2021). Insights into the climate-driven evolution of gas hy-drate-bearing permafrost sediments: implications for prediction of environmental impacts and security of energy in cold regions. *RSC Adv.* 11, 14334–14346. doi:10.1039/d1ra01518d

Fu, J. H., and Zhou, L. F. (2000). Triassic stratigraphic provinces of the southern Qilian basin and their petro-geological features. *Northwest Geosci.* 21, 64–72. cnki:sun:xbfk.0.1998-02-003.

Guo, X. W., and Zhu, Y. H. (2011). Well logging characteristics and evalution of hydrates in Qilian Mountain permafrost. *Geol. Bull. China* 30, 1868–1873. doi:10.3969/j.issn.1671-2552.2011.12.009

He, J. X., Yan, W., Zhu, Y. H., Hu, Y., Zhang, J. R., and Gong, X. F. (2013). Genetic types of gas hydrate in the world and their main controlling factors. *Mar. Geol. Quat. Geol.* 33 (2), 121–128. doi:10.3724/sp.j.1140.2013.02121

Hu, D. G., Zhang, Y. L., and Qi, B. S. (2017). New knowledge obtained from geological survey of gas hydrate in permafrost of Northeast China. *News Lett. China Geol. Surv.* 3, 33–36.

Jia, G. X. (2000). An effective example searching oil-gas fields by using mercury as absorbed state in soil. *Mineral Resour. Geol.* s1, 526–529.

Kvenvolden, K. A. (1993). Gas hydrates—geological perspective and global change. *Rev. Geophys.* 31, 173–187. doi:10.1029/93rg00268

Kvenvolden, K. A. (2022). Methane hydrate in the global organic carbon cycle. *Terra nova.* 14, 302–306. doi:10.1046/j.1365-3121.2002.00414.x

Kvenvolden, K. A., and Lorenson, T. D. (2001). The global occurrence of natural gas hydrate. *Am. Geophys. Union* 124, 3–18. doi:10.1029/gm124p0003

Leeper, J. E. (1981). Mercury corrosion in liquefied natural gas plants. *Energy Process* 73 (3), 46–51.

Li, B., Sun, Y. H., Guo, W., Shan, X. L., Wang, P. K., Pang, S. J., et al. (2017). The mechanism and verification analysis of permafrost-associated gas hydrate formation in the Qilian Mountain, Northwest China. *Mar. Petroleum Geol.* 86, 787–797. doi:10.1016/j.marpetgeo.2017.05.036

Li, C. J., and Ma, S. H. (1999). "Fractal, chaos and ANN," in *Mineral exploration* (Beijing: Geological publishing house).

Li, G. Z., Yuan, Z. Y., Zhuan, Y., and Jiang, H. (2008). Geological significance of mercury element for petroleum exploration. *Geophys. Geochem. Explor.* 32 (2), 143–146. doi:10.1016/S1876-3804(08)60015-4

Li, Q. M., and Cheng, Q. M. (2004). Fractal singular-value (Egin-Value) decomposition method for geophysical and geochemical anomaly reconstruction. *Earth Sci.* 29 (1), 109–118. doi:10.3321/j.issn:1000-2383.2004.01.019

Lin, Z. Z., Kong, G. S., Pan, H. P., Jia, D. Y., Feng, J., and O, Y. (2017). Parameters calculation for the gas hydrate reservoir in Muli area. *Geophys Geochem Explor* 41, 1099–1104. doi:10.11720/wtyht.2017.6.15

Lin, Z. Z., Pan, H. P., Fang, H., Gao, W. L., and Liu, D. M. (2018). High-altitude well log evaluation of a permafrost gas hydrate reservoir in the Muli area of Qinghai, China. *Sci. Rep.* 8, 12596. doi:10.1038/s41598-018-30795-x

Lu, Z. Q., Li, Y. H., Wang, W. C., Liu, C. L., and Wen, H. J. (2015b). Study on the accumulation pattern for permafrost-associated gas hydrate in Sanlutian of Muli, Qinghai. *Geoscience* 29 (5), 1014–1023. doi:10.3969/j.issn.1000-8527.2015.05.004

Lu, Z. Q., Tang, S. Q., Luo, X. L., Zhai, G. Y., Fan, D. W., Liu, H., et al. (2020). A natural gas hydrate-oil-gas system in the Qilian Mountain permafrost area, northeast of Qinghai-Tibet Plateau. *China Geol.* 3, 511–523. doi:10.31035/cg2020075

Lu, Z. Q., Tang, S. Q., Wang, W. C., Tan, P. P., Li, Q. H., Liu, W. J., et al. (2015a). Study on the Nature of the gas source for permafrost associated gas hydrate in Sanlutian of Muli, Qinghai. *Geoscience* 29, 995–1001. doi:10.3969/j.issn.1000-8527.2015.05.002

Lu, Z. Q., Zhu, Y. H., Zhang, Y. Q., Wen, H. J., Li, Y. H., Jia, Z. Y., et al. (2010). Basic geological characteristics of gas hydrates in Qilian Mountain permafrost area, Qinghai Province. *Mineral. Deposits* 29, 182–191. doi:10.1360/972010-741

Lu, Z. Q., Zhu, Y. H., Zhang, Y. Q., Wen, H. J., Li, Y. H., and Liu, C. L. (2011). Gas hydrate occurrences in the Qilian Mountain permafrost, Qinghai province, China. *Cold Reg. Sci. Technol.* 66, 93–104. doi:10.1016/j.coldregions.2011.01.008

Makogon, Y. F., Holditch, S. A., and Makogon, T. Y. (2007). Natural gas hydrates–A potential energy source for the 21st Century. *J. Petroleum Sci. Eng.* 56, 14–31. doi:10.1016/j.petrol.2005.10.009

Ning, F. L., Liang, J. Q., Wu, N. Y., Zhu, Y. H., Wu, S. G., Liu, C. L., et al. (2020). Reservoir characteristics of natural gas hydrates in China. *Nat. Gas. Ind.* 8, 1–24. doi:10.3787/j.issn.1000-0976.2020.08.001

Pan, Y. L., Tian, G. F., Luan, A. H., Xu, N., and Zhao, P. (2008). Application of well logging in frozen earth researches in Muri Coalfield, Qinghai. *Coal Geol. China* 20, 7–13. doi:10.3969/j.issn.1674-1803.2008.12.003

Pang, S. J., Su, X., He, H., Zhao, Q., Zhu, Y. H., and Wang, P. K. (2013). Geological controlling factors of gas hydrate occurrence in Qilian Mountain permafrost, China. *Earth Sci. Front.* 20 (1), 223–239.

Riedel, M., Bellefleur, G., Mair, S., Brent, T., and Dallimore, S. (2009). Acoustic impedance inversion and seismic reflection continuity analysis for delineating gas hydrate resources near the Mallik research sites, Mackenzie Delta, Northwest Territories, Canada. *Geophysics* 74 (5), B125–B137. doi:10.1190/1.3159612

Schmitt, D. R., Welz, M., and Rokosh, C. D. (2005). High-resolution seismic imaging over thick permafrost at the 2002 Mallik drill site. *Bull. Geol. Surv. Can.* 585, 1–13.

Shen, W. (2002). *Fractal chaos and mineral prediction*. Beijing: Geological publishing house.

Sloan, E. D. (2003). Fundamental principles and applications of natural gas hydrates. *Nature* 426, 353–359. doi:10.1038/nature02135

Sun, Z. J., Yang, Z. B., Mei, H., Qin, A. H., Zhang, F. G., Zhou, Y. L., et al. (2014). Geochemical characteristics of the shallow soil above the Muli gas hydrate reservoir in the permafrost region of the Qilian mountains, China. *J. Geochem. Explor.* 139, 160–169. doi:10.1016/j.gexplo.2013.10.006

Tang, R. L., Sun, Z. J., Zhang, S. Y., Li, Q. X., Yang, Z. B., Zhang, F. G., et al. (2016). Halogen elements I and Cl: the exploratory elements of gas hydrate in permafrost area. *Comput. Tech. Geophys. Geochem. Explor.* 38 (4), 553–559. doi:10.3969/j.issn.1001-1749.2016.04.18

Tang, R. L., Xu, J. L., Chen, Z. W., Liu, B., and Bai, J. F. (2023). Inert gas—a new geochemical technology for natural gas hydrate exploration in midlatitude permafrost. *Minerals* 13, 1393. doi:10.3390/min13111393

Wang, C. Q., Ding, Y. Y., Hu, D. G., Qi, B. S., Zhang, Y. L., Tao, T., et al. (2017). Temperature monitoring results for gas hydrate borehole DK-9 and thickness of gas hydrate stability zone in the Qilian Mountains permafrost. *Geoscience* 31, 158–166. doi:10.3969/j.issn.1000-8527.2017.01.014

Wang, P. K., Huang, X., Lu, Z. Q., Pang, S. J., Zhu, Y. H., Zhang, S., et al. (2015). Geochemical dynamics of the gas hydrate system in the Qilian Mountain Permafrost, Qinghai, northwest China. *Mar. Petroleum Geol.* 59, 72–90. doi:10.1016/j.marpetgeo.2014.07.009

Wang, P. K., Zhu, Y. H., Lu, Z. Q., Bai, M. G., Huang, X., Pang, S. J., et al. (2019). Research progress of gas hydrates in the Qilian Mountain permafrost, Qinghai, northwest China: review. *Sci. Sin. Phys. Mech. Astron.* 49, 034606. doi:10.1360/sspma2018-00133

Wang, P. K., Zhu, Y. H., Lu, Z. Q., Guo, X. W., and Huang, X. (2011). Gas hydrate in the Qilian Mountain permafrost and its distribution characteristic. *Geol. Bull. China* 30, 1839–1850.

Wen, H. J., Lu, Z. Q., Li, Y. H., Wang, W. C., Liu, W. J., and Li, X. (2015). New advance on gas hydrate survey and research in sanlutian of Muli, Qinghai. *Geoscience* 29 (5), 983–994. doi:10.3969/j.issn.1000-8527.2015.05.001

Wen, H. J., Shao, L. Y., Li, Y. H., Lu, J., Zhang, S. L., Wang, L. W., et al. (2010). Structure and stratigraphy of the Juhugeng coal district at Muli, Tianjun county, Qinghai province. *Geol. Bull. China* 30, 1823–1828. doi:10.3969/j.issn.1671-2552.2011.12.003

Xie, X. J. (1992). Local and regional surface geochemical exploration for oil and gas. *J. Geochem. Explor.* 42, 25–42. doi:10.1016/0375-6742(92)90048-V

Yang, X., Zhao, Y. F., and Yao, J. Q. (2000). Analysis on Hg anomaly forming mechanism above oil and gas reservoir. *Mineral Resour. Geol.* 14 (6), 397–400. doi:10.3969/j.issn.1001-5663.2000.06.012

Yang, Y. B., Zhang, J. L., and Wu, X. M. (1995). *Petroleum geochemical exploration*. Wuhan: China University of Geosciences Press.

Zhai, G. Y., Lu, Z. Q., Lu, H. L., Zhu, Y. H., Yu, C. Q., and Chen, J. W. (2014). Gas hydrate geological system in the Qilian Mountain permafrost. *Mineral. Petrol* 34 (4), 79–92. doi:10.1007/s00710-013-0321-8

Zhang, F. G., Zhou, Y. L., Zhang, S. Y., Tang, R. L., Wang, H. Y., Sun, Z. J., et al. (2019). Thermal-release mercury-an new tool for natural gas hydrate exploration. *Geophy. Geochem. Explor.* 43 (2), 329–337. doi:10.11720/wtyht.2019.1347

Zhang, F. G., Qin, A. H., Zhu, Y. H., Sun, Z. J., Zhang, S. Y., Wang, H. Y., et al. (2020). A discussion on geochemical migration mechanism of natural gas hydrate in Qilian Mountain permafrost. *Min. Depos.* 39, 326–336. doi:10.1007/s00126-020-00962-1

Zhang, F. G., Sun, Z. J., Yang, Z. B., Zhou, Y. L., Zhang, S. Y., Cao, C. M., et al. (2019). Geochemical investigation of gas hydrate in the permafrost area, China. *Bull. Mineralogy, Petrology Geochem.* 38 (6), 1215–1225. doi:10.19658/j.issn.1007-2802.2019.38.115

Zhang, F. G., Wang, C. W., Zhang, S. Y., Zhou, Y. L., and Tang, R. L. (2018). Hermoluminescence: a new tool for natural gas hydrate exploration. *Geoscience* 32 (5), 1080–1088. doi:10.19657/j.geoscience.1000-8527.2018.05.21

Zhang, F. G., Yang, Z. B., Zhou, Y. L., Zhang, S. Y., and Yu, L. S. (2022). Accumulation mechanism of natural gas hydrate in the Qilian Mountain permafrost, Qinghai, China. *Front. Energy Res.* 10, 1006421. doi:10.3389/fenrg.2022.1006421

Zhang, F. G., Zhou, Y. L., Sun, Z. J., Fang, H., Yang, Z. B., and Zhu, Y. H. (2021). Research progress of geochemical exploration technology for natural gas hydrate in the permafrost area, China. *Adv. Earth Sci.* 36 (3), 6–287. doi:10.11867/j.issn.1001-8166.2021.030

Zhou, Y. L., Yang, Z. B., Zhang, S. Y., Zhang, F. G., Sun, Z. J., and Wang, H. Y. (2021). Study on application mode of headspace gas light hydrocarbon in geochemical exploration of natural gas hydrate in permafrost regions. *Acta Geol. Sin.* 95 (6), 1995–2007. doi:10.1111/1755-6724.14088

Zhou, Y. W., Guo, D. X., Qiu, G. Q., Cheng, G. D., and Li, S. D. (2000). *China permafrost*. Beijing: Science Press.

Zhu, Y. H., Liu, Y. L., and Zhang, Y. Q. (2006). Formation conditions of gas hydrates in permafrost of the Qilian Mountains, Northwest China. *GeolBull China* 25, 58–63. doi:10.3969/j.issn.1671-2552.2006.01.010

Zhu, Y. H., Lu, Z. Q., and Lin, X. L. (2011). Potential distribution of gas hydrate in the Qinghai-Tibetan Plateau. *Geol. Bull. China* 30 (12), 1918–1926. doi:10.1007/s11629-011-1023-0

Zhu, Y. H., Zhang, Y. Q., Wen, H. J., Lu, Z. Q., Jia, Z. Y., Li, Y. H., et al. (2010). Gas hydrates in the Qilian Mountain permafrost, Qinghai, northwest China. *Acta Geol. Sin.* 84, 1–10. doi:10.1111/j.1755-6724.2010.00164.x

Zuo, R. G., and Wang, J. (2015). Fractal/multifractal modeling of geochemical data: a review. *J. Geochem. Explor.* 164, 33–41. doi:10.1016/j.gexplo.2015.04.010